Physical and biological processes over a submarine canyon during an upwelling event

S.E. Allen, C. Vindeirinho, R.E. Thomson, M.G.G. Foreman, and D.L. Mackas

Abstract: Short, shelf-break canyons are shown to have a substantial influence on local water properties and zooplankton distribution. Barkley Canyon (6 km long) off the west coast of Vancouver Island was extensively sampled in July 1997 and found to have water property and current patterns similar to those observed over Astoria Canyon (22 km long) off the coast of Washington State. Results from Barkley Canyon reveal that the canyon influence can occur very close to the surface (at the thermocline depth of 10 m) and that, near the canyon rim, the stretching vorticity generated over the canyon is strong enough to produce a closed cyclonic eddy of sufficient strength to trap deep passively drifting tracers. Most zooplankton species are advected by the currents; those near the ocean surface pass over the canyon, while those at depth are advected toward the coast. Euphausiids (*Euphausia pacifica* and *Thysanoessa spinifera*), the strongest swimming zooplankton collected in the 1997 study, were most prevalent in the closed eddy region near the head of the canyon. The observed aggregation of these animals appears to be linked to their ability to remain at specific depths combined with advection by horizontally convergent flows in the eddy.

Résumé : Les courts canyons sur les bordures escarpées du plateau continental peuvent exercer une grande influence sur les propriétés hydrologiques locales et sur la répartition du zooplancton. Une étude détaillée en juillet 1997 du canyon Barkley (6 km de longueur) au large de la côte occidentale de l'île de Vancouver a révélé que les propriétés hydrologiques et les patterns de courants qui y règnent sont semblables à ceux qui ont été observés au canyon Astoria (22 km de longueur) au large de la côte de l'état du Washington. L'influence du canyon Barkley se manifeste jusque près de la surface (à 10 m, la profondeur de la thermocline); près de la bordure du canyon, l'étirement du tourbillon généré dans le canyon est suffisamment fort pour produire un tourbillon cyclonique fermé assez puissant pour retenir des traceurs qui dérivent passivement en profondeur. La plupart des espèces du zooplancton sont advectées par les courants; celles qui sont près de la surface de l'océan passent au-dessus du canyon, mais celles qui sont plus en profondeur sont advectées vers la côte. Les euphausiidés (*Euphausia pacifica* et *Thysanoessa spinifera*), les meilleurs nageurs dans le zooplancton récolté en 1977, se retrouvent surtout dans la région du tourbillon fermé près du sommet du canyon. La répartition contagieuse de ces animaux semble s'expliquer par leur capacité de se maintenir à des profondeurs particulières, ainsi que par l'advection par les courants horizontaux convergents dans le tourbillon.

[Traduit par la Rédaction]

Introduction

Shelf-break canyons such as Barkley Canyon, located at 48°25′N 126°00′W off the southwest continental margin of Vancouver Island (Fig. 1), are deep (hundreds of metres) and steep-sided valleys that cut from the continental slope into the continental shelf. During upwelling-favourable conditions on the shelf, enhanced upwelling occurs within these canyons (Freeland and Denman 1982; Hickey et al. 1986; Hickey 1997), producing local vertical displacements of various water property isoclines (e.g., temperature, salinity, density, oxygen, nutrient concentration). Local concentrations of plankton and fish are also often enhanced in and around shelf-break canyons (Pereyra et al. 1969; Macquart-Moulin and Patriti 1996; Mackas et al. 1997). In this paper, we use water property, current meter, and zooplankton measurements from Barkley Canyon to define the flow features associated with a canyon during upwelling and to determine the influence of the flow pattern on zooplankton distributions.

Shelf-break canyons vary greatly in size. Compared with Astoria Canyon, for which detailed cross-canyon hydrographic and current measurements have been made during upwelling events (Hickey 1997), Barkley Canyon is short, has less vertical relief, and is somewhat narrower. Barkley Canyon is 13 km wide and 6 km long whereas Astoria Canyon is 16 km wide and 25 km long. The water inshore from Barkley canyon is approximately 150 m deep and the shelf break upstream and downstream of the canyon is about 200 m deep. The water inshore from Astoria Canyon is 75 m deep and the shelf break upstream and downstream of the canyon is about 150 m deep. A water parcel traveling parallel to the shelf break north of Barkley Canyon would encounter maximum depth changes over the canyon of about 400 m. Astoria Can-

Received March 8, 2000. Accepted November 18, 2000. Published on the NRC Research Press Web site on March 16, 2001.
J15657

S.E. Allen[1] and C. Vindeirinho. Oceanography, Department of Earth and Ocean Sciences, University of British Columbia, 6270 University Boulevard, Vancouver, BC V6T 1Z4, Canada.
M.G.G. Foreman, D.L. Mackas, and R.E. Thomson. Institute of Ocean Sciences, P.O. Box 6000, Sidney, BC V8L 4B2, Canada.

[1]Corresponding author (e-mail: allen@ocgy.ubc.ca).

 DOI: 10.1139/cjfas-58-4-671

Fig. 1. Geographical area around Barkley Canyon and the locations of the sampling stations. (*a*) Inset shows the location of the main map relative to Vancouver Island and the Strait of Georgia. The main map shows the location of Barkley Canyon with the locations of the wind buoy, mooring MA1, and hydrographic lines B and C. The bathymetric contours are in metres. The dashed box refers to the area shown in Fig. 1*b*. (*b*) Hydrographic stations sampled around Barkley Canyon in July 1997 (circles and triangles), zooplankton tow stations from July 1997 (triangles), and mooring locations occupied during the summer of 1997 (circled dots). The

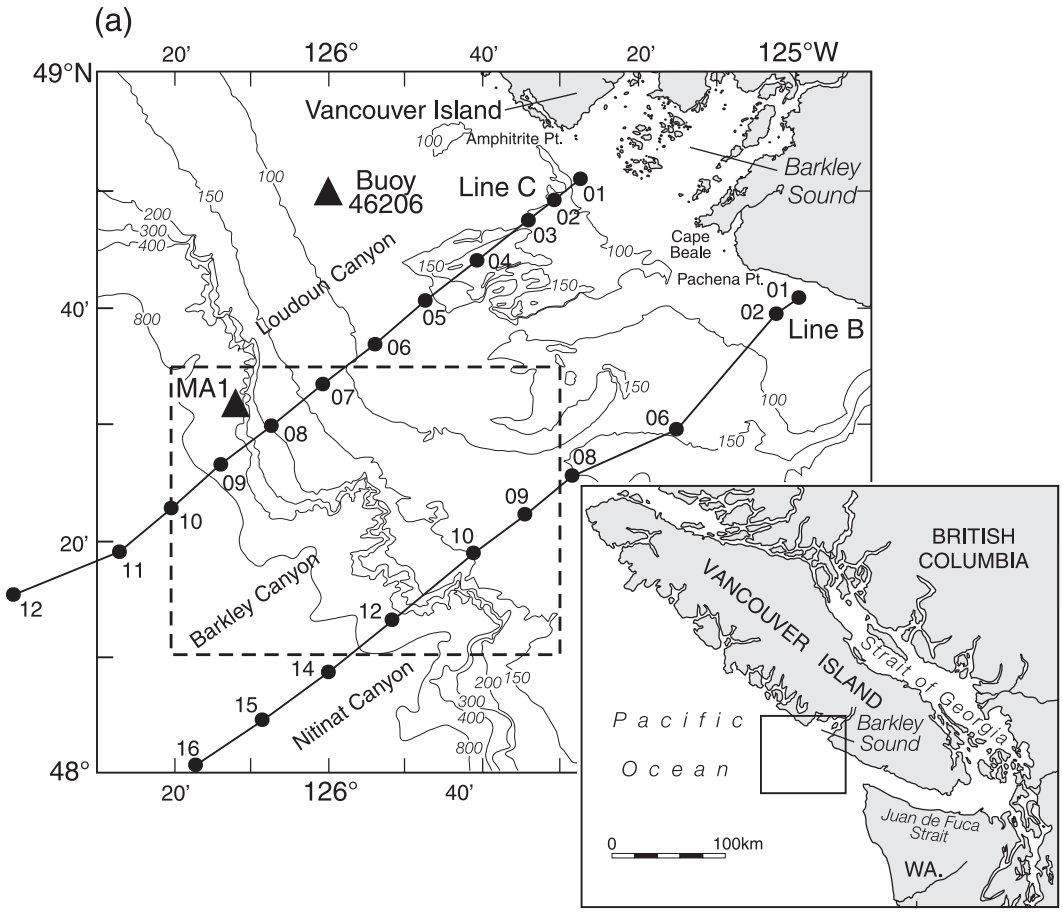

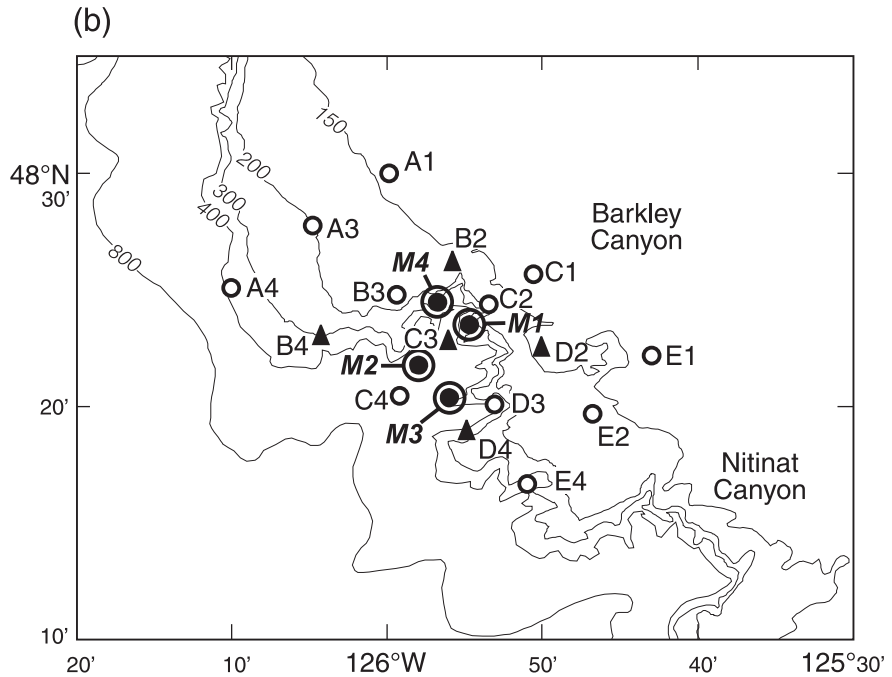

bathymetric contours outline Barkley Canyon and Nitinat Canyon. The shelf break in the vicinity of the canyons occurs at about the 200-m contour. This contour also outlines the rim of the canyons. The region where a canyon opens up onto the continental slope is called the mouth; station C4 marks the centre of the mouth of Barkley Canyon. The region where the canyon merges with continental shelf is called the head; mooring M1 marks the centre of the head of Barkley Canyon. During upwelling-favourable currents, flow is southeastward; upstream is towards the northwest and downstream towards the southeast.

Fig. 2. Schematic of the flow around a submarine canyon during upwelling-favourable conditions from the results of Klinck (1996), Allen (1996), and Hickey (1997), all based on Astoria Canyon. Four depths of flow are sketched. Near-surface flow passes over the canyon unaffected. Flow near the shelf bottom (but above the bottom boundary layer) is advected over the canyon and drops down into the canyon. Stretching generates cyclonic vorticity that turns the flow up canyon. As this flow crosses the downstream rim of the canyon, the fluid columns are compressed and anticyclonic vorticity is generated. Flow over the slope is advected into the canyon and upwelled onto the shelf. Deeper flow over the slope turns cyclonically within the canyon. Typical horizontal scales are 5–30 km for the width and length of the canyon and 300–600 m for the depth. The depth of the shelf is of order 100–200 m.

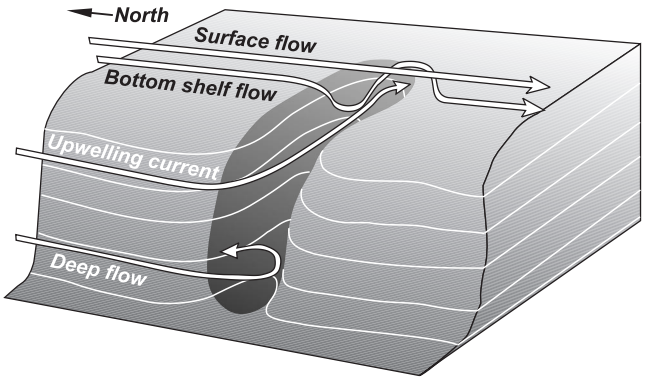

yon cuts further into the shelf than Barkley Canyon (to the 100-m contour) and is significantly deeper. Along the shelf break, depth changes are around 450 m.

Our conceptual model of the flow around a submarine canyon during upwelling has the following main characteristics. During periods of southward along shelf-break flow, enhanced upwelling occurs in west coast canyons. The shelf-break current is in approximate geostrophic balance with a cross-shelf pressure gradient. Within the canyon, the flow along the shelf is inhibited by the canyon walls. The Coriolis force is reduced and the geostrophic balance is upset, producing an unbalanced cross-shore (i.e., up-canyon) pressure gradient (Freeland and Denman 1982). A three-dimensional interpretation of the flow (based on results from Klinck (1996), Allen (1996), and Hickey (1997)) shows that the near-surface flow is unaffected by the canyon and passes straight over it (Fig. 2). Deep within the canyon, the initial flow towards the head of the canyon causes the isopycnals to tilt up towards the canyon head, which in turn tends to balance the overlying barotropic pressure gradient, reducing the up-canyon flow (Allen 1996). The flow is trapped within the canyon. The lifted isopycnals induce vortex stretching, which causes cyclonic vorticity in the deep layer (Hickey 1997).

Flow near the canyon rim is strongly influenced by nonlinear advective effects (Allen 1996). As the flow near the level of the rim passes over the upstream wall of the canyon, it tends to descend into the canyon and be stretched (Hickey 1997). The vorticity generated during this process turns the flow up canyon. As the flow crosses the downstream rim, anticyclonic vorticity is generated (Allen 1996). Some flow from the slope is advected into the canyon and then up and onto the shelf at the downstream wall of the canyon near the head. Most flow from the slope continues downstream past the mouth of the canyon (Klinck 1996).

The complicated flow structure around canyons imply onshore advection of any small, weakly motile zooplankton that permanently inhabit the 150- to 400-m depth stratum and probable complex effects when combined with the swimming behaviour of larger, more motile and vertically migrating macrozooplankton. Diel vertically migrating zooplankton have been observed to concentrate around canyon heads and on upper-slope bottoms (Macquart-Moulin and Patriti 1996). Acoustic backscatter observations of euphausiids around a shelf break and canyon have shown aggregation proportional to the strength of cross-isobath flow (Mackas et al. 1997). The presence of increased zooplankton abundance within canyons is consistent with evidence of increased concentrations of fish (Pereyra et al. 1969; Mackas et al. 1997) and whales (Whitehead et al. 1997).

After the methods of data collection and analysis are presented, the physical and biological observations over Barkley Canyon are given. We show that Barkley Canyon has flow characteristics very similar to those of Astoria Canyon during upwelling conditions. Our observations imply effects of the canyon near to the ocean surface that may directly influence primary productivity in the region. Weakly motile zooplankton are shown to be advected with the currents whereas euphausiids are shown to be aggregated in horizontal flow convergences (at their deep daytime depth).

Methods

Observations over Astoria Canyon (Hickey 1997) revealed variability of the flow field at remarkably small spatial scales (vertical and horizontal scales of 40 and 500 m, respectively). These observations show that, in order to interpret the motions within the canyon in terms of theory, it is necessary to acquire flow and density field information from continental shelf and slope locations upstream of the canyon. As part of the Canadian Global Ocean Ecosystems Dynamics Program (GLOBEC), we collected conductivity–temperature–depth (CTD) profiles at 16 closely spaced locations in the immediate vicinity of Barkley Canyon (Fig. 1*b*) as well as more widely spaced CTD profiles from the time series grid extending across the shelf from north of Brooks Peninsula (450 km north of the canyon) to the U.S.–Canada border (80 km south of the canyon). The CTD profiles included transmissionmeter data, which we used to index concentration and depth distribution of small suspended particulates (mostly phytoplankton). Four moorings were positioned within the canyon (Fig. 1*b*) and a fifth mooring, MA1, was located 30 km north of the canyon over the shelf break (Fig. 1*a*). Mooring MA1 has been maintained for 15 years and is used to characterize the shelf/slope circulation (Thomson and Ware

Table 1. Index of shelf versus offshore distribution affinities for the zooplankton taxa examined in this study.

Taxon	Major group	May–June	July	Aug.–Sept.	Average
Oikopleura	Larvacean	–0.63	–0.47	–0.73	–0.61
Thysanoessa spinifera	Euphausiid	–1.25	–0.30	–0.20	–0.58
Acartia longiremis	Copepod	–0.46	–0.66	–0.20	–0.44
Sagitta elegans	Chaetognath	–0.54	–0.08	–0.05	–0.23
Pseudocalanus spp.	Copepod	–0.07	–0.14	–0.18	–0.13
Paracalanus parvus	Copepod	0.04	0.02	–0.38	–0.11
Euphausiid larvae (both *Euphausia pacifica* and *Thysanoessa spinifera*)	Euphausiid	–0.20	–0.12	0.04	–0.09
Calanus marshallae	Copepod	–0.42	0.44	0.14	0.05
Oithona spp.	Copepod	0.37	0.56	0.41	0.45
Metridia pacifica	Copepod	0.36	0.71	0.71	0.59
Euphausia pacifica	Euphausiid	0.49	1.10	0.72	0.77
Eukrohnia hamata	Chaetognath	1.22	1.42	1.66	1.44
Neocalanus plumchrus	Copepod	1.05	2.11	2.03	1.73
Sagitta scrippsae	Chaetognath	2.41	4.08	2.18	2.89

Note: Rows (taxa) are ranked from most "nearshore" to most "offshore." Columns indicate the evolution of this pattern with season. Negative entries in the table indicate higher biomass on the shelf, positive values indicate higher biomass seaward of the shelf break, and near-zero values indicate similar biomass at shelf and slope locations. The index is computed from 1979–1991 seasonal climatologies reported in Mackas (1992). For each time period and taxon, the index = log(average shelf biomass/average offshore biomass).

1996). Hourly wind data were acquired from a permanent weather buoy maintained by the Meteorological Service of Canada seaward of Barkley Sound (buoy 46206: 48°50′N, 126°W; Fig. 1*a*). The weather buoy reports hourly values of wind direction and vector-averaged wind speed.

The Barkley Canyon CTD and zooplankton data were acquired during July 25–27, 1997. CTD casts were performed at each of the 16 stations (Fig. 1*b*) with two additional profiles taken at stations B4 and C4 and three extra profiles at station D4 (for time series considerations). The CTD data were despiked and binned into 1-m depth intervals. Coincident water bottle samples taken from the rosette were used to validate the manufacturer's (Seabird Electronics) specified accuracies of 0.003 (salinity), 0.001°C (temperature), and 0.15% full-scale pressure.

Zooplankton distributions (shallow versus full water column and daylight versus night) were compared among five of the CTD sampling locations (Fig. 1*b*). Two of the stations (B4, D4) were close to the walls at the mouth of the canyon, one (C3) was in the centre of the canyon, and the last two (B2, D2) were at the head of the canyon on the shelf. The basic sampling design was a set of four bongo vertical net tows at each of these sites: one visit during daylight and one during the night and, at each visit, one "shallow" tow from 50 m to the surface and one "deep" tow (from 250 m to the surface at the three deeper sites, from approximately 15 m above the bottom to the surface at B2 and D2). The 50-m night tow at station D2 was missed. Bongo nets had a diameter of 0.56 cm and a mesh size of 236 µm. Animals were preserved in buffered 5% formalin solution and returned to the laboratory for identification and enumeration of selected taxa (Table 1).

The taxa selected for analysis included species that were dominant within the local zooplankton community during the preceding decade (Mackas 1992) but were also selected to include a range of body size, migratory strategy, and shelf versus oceanic primary habitat. Large copepods were represented by the genera *Neocalanus* and *Calanus*, small copepods by *Paracalanus*, *Pseudocalanus*, *Acartia*, and *Oithona*, chaetognaths by *Sagitta* and *Eukrohnia*, euphausiids by *Euphausia* and *Thysanoessa*, and larvaceans by *Oikopleura*. The species were divided into groups based on three criteria: (*i*) their usual cross-shore location in the southern section of the Vancouver Island continental margin (shelf, shelf edge, or oceanic) (Table 1) (Mackas 1992; Peterson et al. 1979), (*ii*) whether they usually follow a diel migration pattern (migrators or nonmigrators), and (*iii*) whether they were found predominantly above or below 50 m (shallow, deep, or mixed). For each species at each time (day or night) and for each depth of tow, the number of animals per square metre was calculated by dividing the total catch per sample by the volume filtered (from the flow meter) and then multiplying by the vertical range of the tow.

Four Aanderaa RCM4 moorings (Fig. 1*b*) were positioned in the canyon. They were deployed on April 19, 1997, at M2, M3, and M4 and on June 4 at M1. All moorings were recovered on October 2. All instruments recorded half-hourly values of currents, temperature, and salinity. At sites M1 and M3, three RCM4s were placed at depths of 150, 250, and 350 m. Instrument depths were 250 and 350 m at M2 and 250 m at M4. All time series data from the moorings were filtered (detided) using a squared eighth-order Butterworth filter with a 40-h cutoff. According to the manufacturer's specifications, the RCM4s have resolutions of 0.3°C and 0.05 (salinity). The threshold of the current meters is roughly 2 $cm \cdot s^{-1}$ and speeds are accurate to within 1 $cm \cdot s^{-1}$ or 2% of the actual speed, whichever is greater. Directions are accurate to 5° for speeds in the range 5–100 $cm \cdot s^{-1}$.

Diagnostic model

The diagnostic, finite-element model FUNDY5 (Lynch et al. 1992; Naimie et al. 1994) was used to estimate the three-dimensional flow fields at the time of the CTD measurements. Horizontal model resolution varied from approximately 8 km in regions with depths greater than 2000 m to less than 400 m along the shelf break and around Barkley Canyon. Linear basis functions were used to approximate all variables, and under each horizontal node, there were 41 vertical nodes whose sinusoidal spacing is similar to that described in Lynch et al. (1996). Similar to the application described in Foreman et al. (2000), the tidal constituents M_2, S_2, K_1, and O_1 were also included in the computation. They account for approximately 65% of the total tidal speeds near Barkley Canyon.

The combined buoyancy- and wind-driven flows were forced with the average July 25–27 winds measured at buoy 42606 and a three-dimensional density field that was constructed through Kriging of the CTD measurements. Boundary conditions for these calculations were computed through a combination of geostrophic radiation conditions and adjustments to the surface elevations so that the vertically averaged flow passed through the boundary without any reflection. Analogous to the inversion described in

Fig. 3. Conditions during the summer of 1997. All time series were filtered with a squared eighth-order Butterworth filter with a 40-h cutoff. (*a*) Winds at buoy 46206. Summer upwelling-favourable winds (southeastward) prevailed from early June to mid-August. (*b*) Currents at 97 m at mooring MA1. The summer, southward shelf-break current was observed from mid-June until mid-August. (*c*) Temperature at 97 m at MA1. Periods of strong upwelling (sharply decreasing temperature) occurred in mid-June and early August. Weak upwelling (slowly decreasing temperature) occurred in mid-July prior to the time of the cruise (July 25–27, 1997).

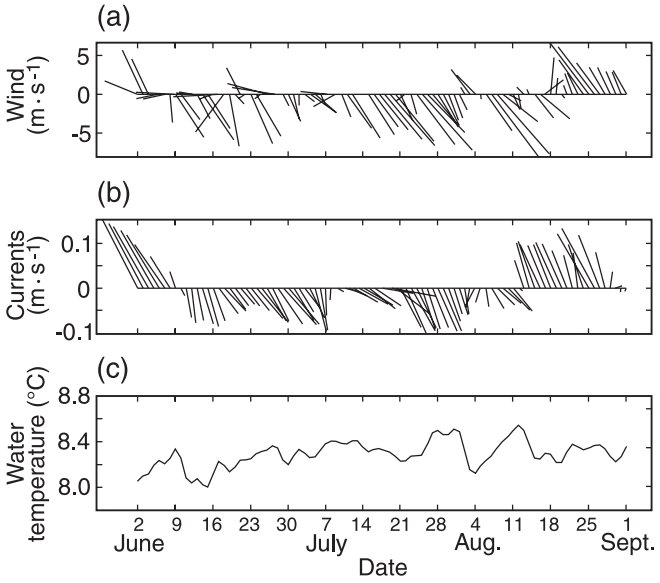

Foreman et al. (2000), further boundary adjustments were also made to balance the estuarine flow in Juan de Fuca Strait and to produce a California Undercurrent consistent with the observations at mooring MA1 (Fig. 1*a*) and mooring ME03, another mooring further north along the shelf break. Because the mooring data indicated that both the meteorological and the flow fields were relatively stationary during the July 1997 GLOBEC cruise, the complete set of late-July density profiles was assumed to be synoptic for the purpose of this model calculation.

Several Lagrangian tracer experiments were carried out with the code DROG3D (Blanton 1992). This software uses a fourth-order Runge–Kutta scheme (Press et al. 1986) to advect tracers through a three-dimensional finite-element grid in a manner consistent with one or more specified current fields. In this case, five current fields were employed: one for each of the four tidal constituents and one for the buoyancy- and wind-driven flows. Although realistic biological behaviour can be incorporated into these calculations, for all our experiments, the tracers were completely passive. (See Smith et al. (2001) for an application that assumes diel vertical migration.)

Results

Regional conditions

Typical summer conditions off the coast of Vancouver Island are characterized by strong northwesterly, upwelling-favourable winds, cold near-surface water temperatures associated with upwelling, and high primary and secondary productivity. Compared with this typical condition, 1997 was an atypical year with weak winds and warm ocean temperatures because of the strong El Niño of 1997–1998 (Freeland and Thomson 1999). During the summer and autumn of 1997, a major near-surface coastal warming event occurred throughout the Northeast Pacific (Freeland and Thomson 1999). In particular, temperatures at 32 m depth at mooring MA1 were 6°C above normal. It is postulated that this warming was due to atmospheric teleconnections (Freeland and Thomson 1999), which is consistent with the observed wind anomalies.

Although summer upwelling in 1997 was generally weaker than normal, winds from a buoy off Barkley Sound (Fig. 3*a*) show periods of strong (5 $m \cdot s^{-1}$) northwesterly, upwelling-favourable winds. Currents above 200 m at mooring MA1, 30 km north of Barkley Canyon, were northwestward during June with a sharp change to southeastward flow (typical summer conditions) in mid-June (Fig. 3*b*). The temperature at mooring MA1 at 97 m depth (Fig. 3*c*) indicates strong upwelling in early June and in early August and weaker upwelling from mid- to late July.

The CTD data over the canyon were collected during July 25–27 during a period of sustained moderate to strong northwesterly winds (Fig. 3*a*). At mooring MA1 at 97 m depth, an intensification of southeastward flow began at about July 21. Relatively weak upwelling was observed along line C just north of the canyon. Along this line, the 24 sigma-*t* surface shoaled from 30 m offshore to 8 m over the shelf break and 12 m nearshore.

Large-scale horizontal distributions of nutrient and chlorophyll were typical for the summer season, although chlorophyll levels were generally low (S. Harris, Oceanography, University of British Columbia, Vancouver, BC V6T 1Z4, Canada, personal communication). Nutrients and chlorophyll were high near the coast and decreased offshore. The higher coastal concentrations are probably related to the estuarine outflow from Juan de Fuca Strait, which transports nutrients onto the southern end of the Vancouver Island shelf (Mackas et al. 1980; Crawford and Dewey 1989) and then continues northward as the coastally trapped Vancouver Island Coastal Current (Thomson et al. 1989).

In summary, during the 1997 Barkley Canyon sampling, the winds were persistently from the north, the shelf-break current was to the south and intensifying, and upwelling over the shelf break was weak.

Water properties over the canyon

Temperature and conductivity profiles from the 16 stations over the canyon give insight into the three-dimensional structure of the isopycnal surfaces. As lines B and C from the large-scale survey are in the vicinity of the canyon, the ends of these lines are included in this analysis.

The depth of the 24 sigma-*t* surface provides a good indication of the thickness of the surface mixed layer and the depth of the underlying seasonal pycnocline. Compared with offshore sampling locations, this surface is raised by 9 m over the shelf break and canyon (Fig. 4*a*). The timing of the canyon stations was carefully examined to ensure that the observed pattern could not be due to aliasing of displacements by internal tide motions. When examined as functions of time, the isopycnal depths showed no evidence of a 12-h tidal period.

A within-canyon vertical displacement of density surfaces is also evident deeper in the water column (Fig. 4*b*). Above the level of the shelf break at a depth of about 150 m, the

Fig. 4. (*a*) Depth of the 24.0 sigma-*t* surface in the vicinity of Barkley Canyon. This isopycnal is within the seasonal thermocline and provides a good indication of the depth of the mixed layer. The positions of the casts are marked with circles. Yellow and red colours outline the region of the raised pycnocline (indicative of upwelling) over the shelf break and over Barkley Canyon. The white regions are unsampled (further than 4 km from any cast). The interpolation is Gaussian with a 2.5-km standard deviation. The standard deviation was chosen to be about the minimum distance between casts so that the result of every cast is evident. The cutoff distance was chosen to be

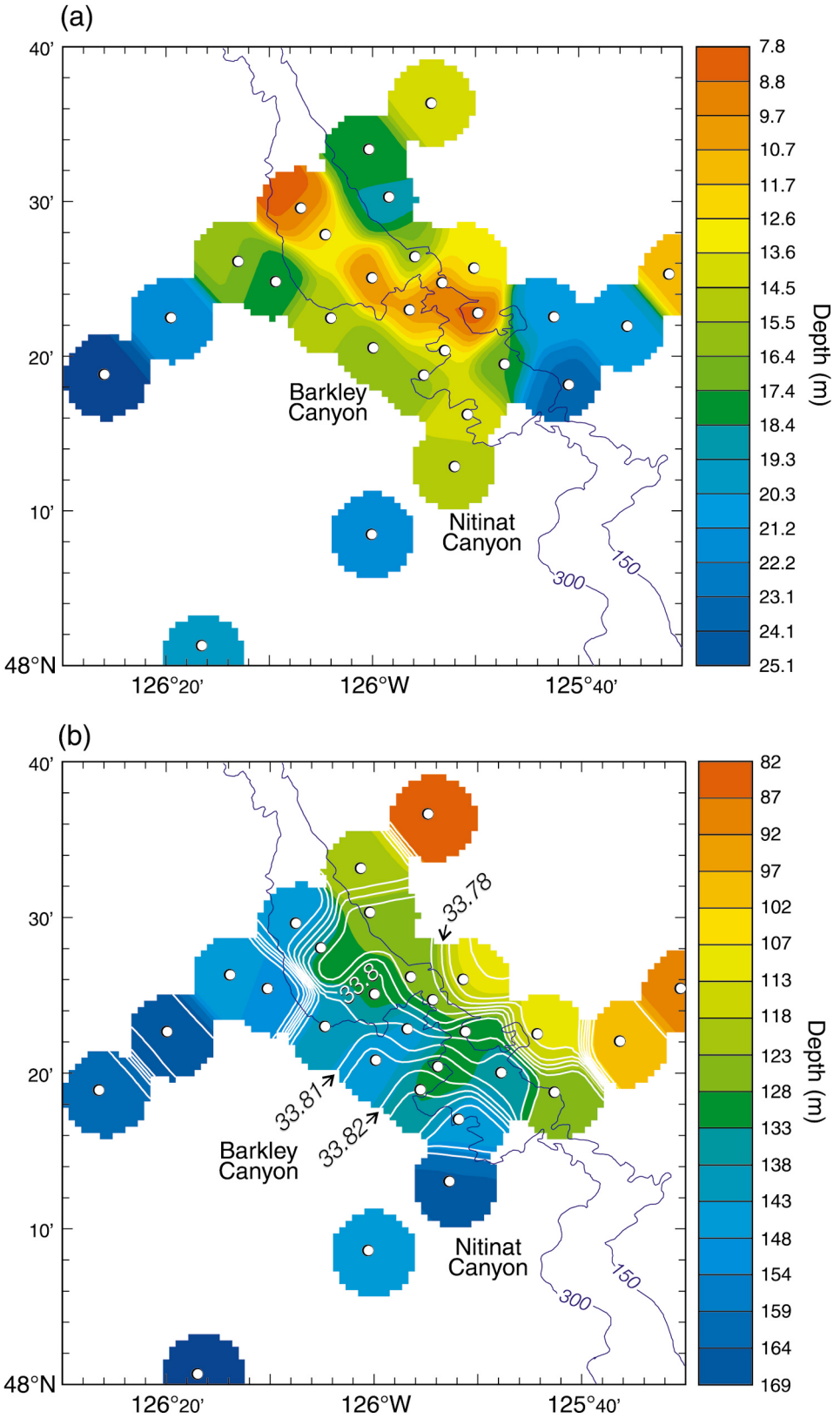

the horizontal length scale in the vicinity of the canyon, about the half width of the canyon. (*b*) Depth of the 26.4 sigma-*t* surface in the vicinity of Barkley Canyon. This isopycnal is about 50 m above rim depth (200 m) over Barkley Canyon. The positions of the casts are marked with circles. This surface is deep (dark blue colour) over the ocean and tilts upwards over the shelf (yellow, orange, and red colours). The surface is elevated (greener) over the edges of the canyon and dips over the canyon (bluer). Over the downstream rim of the canyon. this isopycnal is elevated by about 15 m compared with its level at comparable depths elsewhere in the canyon sampling. This elevation reflects upwelling over the downstream portion of the canyon head. The white lines are contours of salinity on this surface (contoured from 33.745 to 33.865 by 0.005). The salinity contours over the canyon (e.g., 33.81, 33.82) cross the isobaths along the downstream rim of the canyon, again suggesting upwelling there. The white regions are unsampled (further than 4 km from any cast). The interpolation is Gaussian with a 2.5-km standard deviation.

Fig. 5. Averaged (over July 25) filtered currents in the canyon. The thin arrows are currents at 150 m, the open-headed arrows are currents at 250 m, and the solid-headed arrows are currents at 350 m. Flow at 150 m depth is southward and slightly up canyon at mooring M3 and strongly up canyon at M1. At 250 m depth, the flow is primarily cyclonic (currents at M1 probably reflect the local bathymetry). At 350 m depth, the flow is very weak. This flow pattern is consistent with flow over and shorewards (suggesting upwelling) at 150 m (above the canyon rim at 200 m depth), strong cyclonic flow at 250 m (just below the depth of the canyon rim), and weak flow deep in the canyon. Such a flow pattern is consistent with observations and theory for Astoria Canyon.

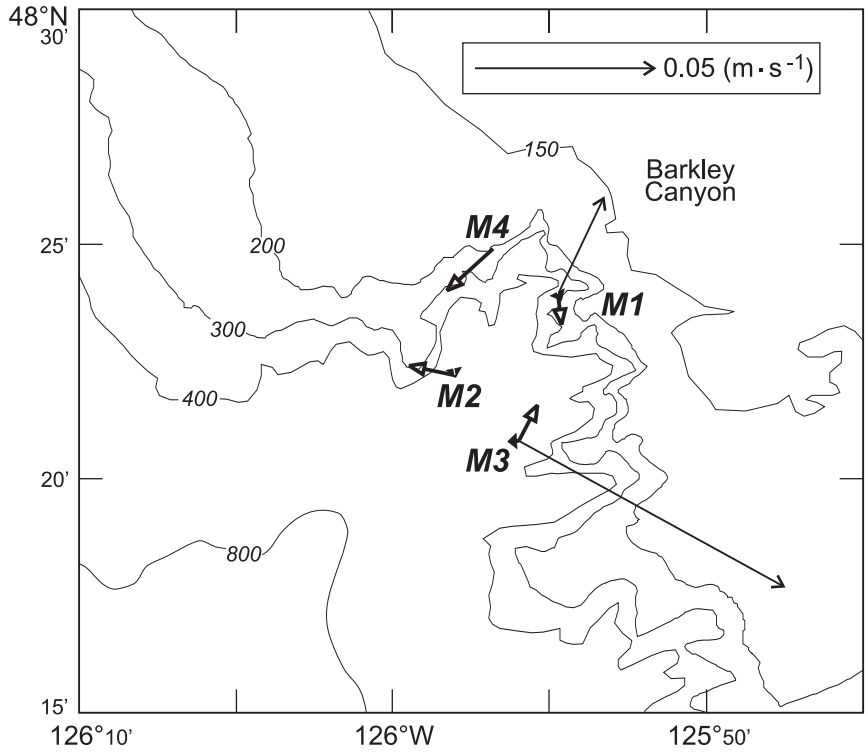

isopycnals are shallower over the upstream and downstream rims of the canyon but dip over the canyon itself. Away from the canyon, the relatively deep 26.4 sigma-*t* isopycnal surface tips strongly up towards the shore, rising from 165 m at station 10 on line C in 1240 m of water to 85 m at station 06 on line C in 92 m of water (see Fig. 1*a* for location of lines B and C). A similar gradient is seen along line B. Within the canyon, this isopycnal is deeper than it is over the two surrounding ridges and is only slightly shallower within the canyon than at a similar depth at line C. Over the downstream rim of the canyon, the 26.4 sigma-*t* surface is elevated by roughly 15 m compared with its level at comparable depths elsewhere in the canyon sampling.

Deeper isopycnals (sigma-*t* 26.6–26.65 lying around 150–250 m depth, not shown) are shallower over the canyon than on the surrounding shelf break, but only by 20 m. The strongest feature in these isopycnals is the cross-shelf tilt, with the stations over the shelf having isopycnals almost 100 m shallower those over the deep ocean. For isopycnals below the rim of the canyon lying between 250 and 350 m depth, there is also strong cross-shelf tilt. Within the canyon, the isopycnals near the centre of the canyon are depressed, giving a "bowl shape" to the isopycnals. Below 350 m depth, the isopycnals vary by about 50 m over the survey domain and the pattern of variation changes rapidly from isopycnal to isopycnal.

The geostrophic flow associated with the density field is described in the next section. If the flow is steady through time, the distribution of properties along isopycnal surfaces can be used as tracers indicating flow patterns. Contours of salinity on the 26.4 sigma-*t* surface cross the downstream rim of the canyon towards the head (Fig. 4*b*). If these are coincident with streamlines (as they would be in steady flow in the absence of mixing), they show strong flow over the

Fig. 6. Currents at 150 m from a diagnostic finite-element model based on the CTD data. The model includes a mean flow and the four major tidal constituents and was forced with the observed density field and averaged winds from buoy 42606. See text for details. The currents from the current meters (shown inside the circles) are superimposed on the modeled flow. Agreement between the model currents and the current meter currents is good. The flow at 150 m forms a strong cyclonic eddy at the head of the canyon above the depth of the rim (200 m). This eddy is strong enough to trap passive tracers, and the convergence regions (e.g., at 48°25′N, 125°57′W) can aggregate depth-maintaining tracers. The strong up-canyon flow through the centre of the canyon (depth greater than 500 m) and onto the shelf is consistent with the observed tendency for deep, weakly motile zooplankton to be advected onshore over the canyon, particularly over the downstream side of the canyon. Peak currents are modeled to be 30 $cm \cdot s^{-1}$ and the vorticity is of order 0.3*f*.

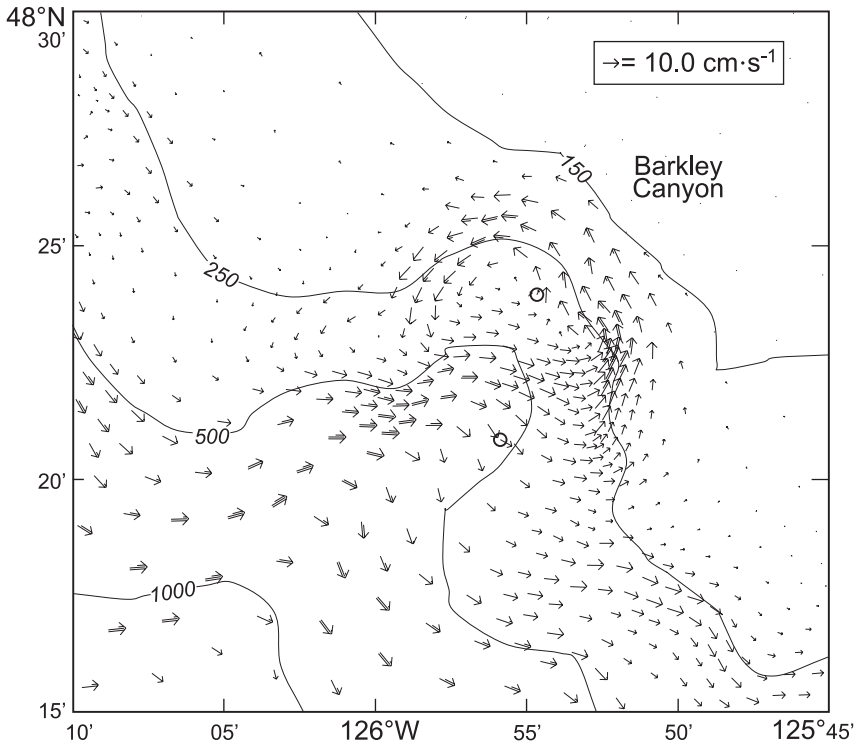

downstream side of the head. The contours of salinity on the 26.62 sigma-*t* surface do not tend to cross the canyon wall but show higher salinity water within the canyon.

The four moorings in the canyon measured the time evolution of the water properties at three depths (350, 250, and 150 m). The time evolution at each depth was different. At the deepest instruments (350 m), changes in temperature, salinity, and density in late July were small. At 250 m, density and salinity peaked in the middle of July 25, with temperature decreasing through the end of the day. Over the 2-day span of July 23–25, sigma-*t* increased by 0.02–0.04. At 150 m, only one conductivity sensor functioned. Temperature decreased sharply by more than $0.1°C \cdot day^{-1}$ from July 23 through to July 26. These observations provide evidence of the upwelling at 150 m depth and the cessation of upwelling at 250 m depth and no evidence of upwelling at 350 m depth.

Currents within the canyon

The residual (detided) currents within the canyon for July 25 (the date of the CTD survey over the canyon) are shown in Fig. 5. The flow at 350 m depth was weak and seaward within the canyon. Except at M1, flow at 250 m depth shows the theoretically expected cyclonic circulation within the canyon. At mooring M3, currents at 150 m show the expected alongshore flow across the topography. However, currents at M1 were oriented much more up canyon than expected.

A detailed picture of the three-dimensional flow was determined from the CTD measurements using the finite-element diagnostic model. At 30 m (not shown), the buoyancy-driven and wind-driven current followed the shelf break in a southeastward direction. Interaction with the bathymetry caused the current to bend, to cross the isobaths, and to turn cyclonically over the canyon heads. The model output for the horizontal velocity at 150 m depth (Fig. 6) shows a fully developed cyclonic eddy over the head of Barkley Canyon. This eddy is well resolved by the four CTD stations at the head of the canyon. Current vectors from the two current meters at this depth are superimposed in the figure. The measured currents agree well with the modeled flow.

Particulates above the canyon

The percent transmission data were used to determine the particulate concentration, *p*, over the canyon from

$$(1) \qquad p = -4.0\ m^{-1} \ln\left(\frac{\%\ \text{transmission}}{92\%}\right)$$

where 92% was the observed clear-water transmission over the 25-cm path length of the transmissometer. The 0- to 50-m vertically integrated particulate concentration was higher over the shelf than over the deep ocean by a factor of about

Table 2. Zooplankton distribution.

Taxon	Depth (m)		B2 (m^{-2})	D2 (m^{-2})	B4 (m^{-2})	D4 (m^{-2})
Oikopleura	0–50	Day	4 800	2 800	5 300	11 000
		Night	910	No data	7 300	510
Thysanoessa spinifera	0–250	Day	61	2.7	0	0
		Night	360	58	6.9	9.3
Acartia longiremis	0–50	Day	7 000	3 400	3 400	2 500
		Night	4 800	No data	890	1 000
Sagitta elegans	0–250	Day	370	49	140	230
		Night	480	190	55	230
Paracalanus parvus	0–50	Day	40 000	29 000	95 000	81 000
		Night	27 000	No data	43 000	27 000
Euphausiid larvae (both *Euphausia pacifica* and *Thysanoessa spinifera*)	0–50	Day	5 500	490	2 800	3 300
		Night	910	No data	1 300	170
Calanus marshallae	0–250	Day	7 400	8 600	0	230
		Night	5 500	5 100	780	2 700
Oithona spp.	0–50	Day	15 000	6 800	25 000	29 000
		Night	1 700	No data	9 700	3 900
Metridia pacifica	0–250	Day	0	180	0	470
		Night	210	0	220	3 600
Euphausia pacifica	0–250	Day	690	19	71	120
		Night	620	270	130	270
Eukrohnia hamata	0–250	Day	46	2.7	120	290
		Night	13	39	35	190
Neocalanus plumchrus	0–250	Day	0	0	1 700	700
		Night	0	470	0	590
Sagitta scrippsae	0–250	Day	77	25	58	73
		Night	26	49	14	93

Note: Station B2 is located at the head of Barkley Canyon on the upstream side. The day samples were collected at 19:12 PDT on July 25 and the night samples were collected at 00:00 PDT on July 26. D2 is located at the head of the canyon on the downstream side (day: 08:11 on July 25; night 02:48 on July 25). B4 is located at the mouth on the upstream side (day: 14:57 on July 25; night 22:49 on July 25). D4 is located at the mouth on the downstream side (day: 16:24 on July 25; night 00:21 on July 25).

2. The canyon was a region of slightly lower numbers of particulates than the nearby slope by about 10%.

All stations had low transmission near the surface. The four ocean stations (ends of lines B and C) also had a second minimum in transmission at 40 m depth. The depth of the bottom of the surface layer varied over the domain and was distinctly shallower over the canyon with the same pattern as that of the depth of the pycnocline (Fig. 4*a*).

Zooplankton distribution

Vertically integrated zooplankton abundances of most species were significantly lower in the centre of the canyon (station C3) than at the stations around the edge of the canyon. (The one exception was *Pseudocalanus* spp., which was abundant both at the canyon axis (C3) and in the eddy region (B2).) Table 2 gives the number of animals per square metre for the dominant genera at each of the four canyon margin stations.

Four species were shallow nonmigrators (*Acartia longiremis*, *Oikopleura* spp., *Oithona* spp., and *Paracalanus parvus*). As these species were presumably equally well sampled by the 50- and 250-m (or deep) tows, these pairs of tows can be used to assess sampling variability. The standard deviation of the distribution was found to be 10%; this number includes counting variations and some estimate of patchiness.

Discussion

In this section, we compare the water property results from Barkley Canyon with our conceptual model of flow around a submarine canyon noted in the Introduction and then interpret the observed zooplankton distribution in terms of how these flow fields advect zooplankton across and through the canyon. As the eddy observed over Barkley Canyon is stronger than those observed above other canyons, we explain the dynamics of its formation. The mechanism by which this eddy causes the observed aggregation of euphausiids is discussed.

Comparison of observed and theoretical currents and water property distributions

The July 1997 observations support the dynamic theory that upwelling within Barkley Canyon is maintained by a cross-shore pressure gradient. To show this, we note that the residual currents are approximately geostrophic so that the geostrophic velocity above the rim of the canyon provides a measure of the cross-shore pressure gradient. Consequently, the alongshore velocity measured at 97 m depth at mooring MA1 should be directly proportional to the cross-shore pressure gradient at the same depth. Similarly, the vertical displacement of isotherms at the head of the canyon is a measure of upwelling within the canyon. Over the 6-month deployment of the moorings, the changes in temperature produced by vertical displacement of isotherms (upwelling within the canyon) were strongly correlated with the 97-m alongshore current (cross-shore pressure gradient; Fig. 7). The correlation between variations in the alongshore cur-

Fig. 7. Alongshore velocity (solid line) at 97 m at mooring MA1 through the summer of 1997 plotted with the temperature (dashed line) at 230 m at M1. As the flow is to first-order geostrophic, the alongshore velocity is proportional to the cross-shore pressure. The vertical displacement of isotherms (a measure of upwelling) is proportional to changes in temperature. The strong correlation between the alongshore velocity and the temperature supports the theory that cross-shore pressure controls the strength of upwelling.

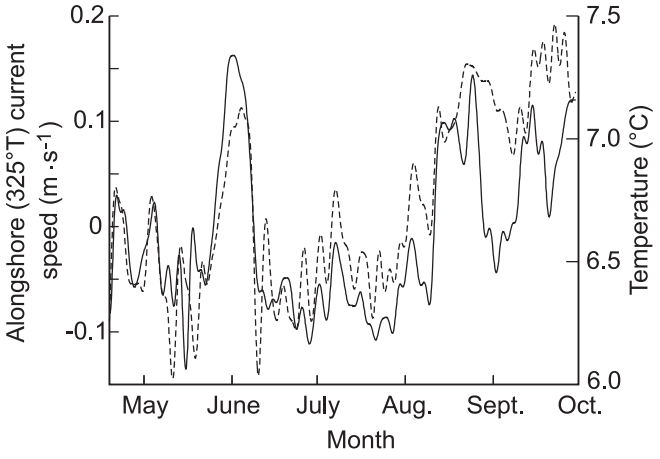

rents at MA1 and temperatures at the head of the canyon at all depths (150, 250, and 350 m) is greater than 0.7.

We did not collect current meter observations above 150 m in 1997, but the diagnostic model forced by observed density fields showed only weak deflections of the currents over the canyon, consistent with numerical predictions and Astoria Canyon observations. The CTD observations, however, show near-surface effects in the form of a strongly raised seasonal pycnocline that is neither predicted by the prognostic numerical models (Allen 1996; Klinck 1996) nor observed over Astoria Canyon (Hickey 1997). The surface layer containing high particulate concentration is thinned by the raised pycnocline. As the height from the pycnocline to the surface is halved over the canyon, the raised pycnocline could significantly increase the rate of entrainment into the mixed layer above and also elevate the subpycnocline water into the euphotic zone. Both processes would act to raise euphotic zone nutrient availability and phytoplankton productivity at the shelf break and over the canyon. Nutrient samples were not available at the canyon stations. Nutrients at station 08 on line C at the shelf break were neither anomalously high nor associated with increased chlorophyll levels. The lack of a definitive canyon-induced nutrient anomaly is probably due to the overriding effect of strong coastal nutrient input in this area from the nearby Vancouver Island Coastal Current and regional coastal upwelling. The raised pycnocline and associated raised particulate layer would imply enhanced productivity both above and below the pycnocline layer. The lack of an observed increase in particulates may be due to the high rate of horizontal advection through this area. A near-surface particle would be swept out of the region in about half a day, which is only about 30–50% of the expected phytoplankton doubling time scale. Thus, particles are swept out of the region before they can significantly contribute to increased biomass.

Very deep within the canyon (350 m), the flow was cyclonic but weak, the isopycnals were nearly level, and no upwelling (temperature decrease with time) was occurring. As the upwelling-favourable flow at 97 m at MA1 during late July was weak and nearly constant, active upwelling deep in the canyon was apparently not occurring. It would appear that a depth of 350 m was below the level of strongly cyclonic flow in Barkley Canyon.

At intermediate depth within the canyon (250 m), the flow was cyclonic, the isopycnals were bowed downwards, and upwelling (higher salinity, lower temperature) had occurred but was ceasing. These observations are consistent with the theoretically modeled deep flow shown schematically in this study.

At near-rim depth (150 m), the observations are in general agreement with previous knowledge except for the presence of the strong eddy. Cyclonic circulation at the rim of the canyon was also seen over Astoria Canyon (Hickey 1997) but only during relaxation of upwelling. Numerical models have predicted cyclonic vorticity but not a closed eddy (Allen 1996; Klinck 1996). The flow at 150 m over Barkley Canyon is consistent with the midlevel flow pattern based on theoretical modeling studies and shown schematically in this study. Salinity contours crossed isobaths and temperature was decreasing, suggesting that upwelling was occurring at this level. The shape of the isopycnal surfaces at this depth (high downstream of the canyon) is consistent with flow up canyon.

In summary, Barkley Canyon has a substantial influence on currents and water property distributions during upwelling similar to that observed over a much longer canyon (Astoria Canyon) to the south. At the start of the canyon field survey (July 25), water at 150 m depth was flowing coastward up the canyon and upwelling over the downstream rim of the canyon. At 250 m depth, upwelling was ceasing and the water recirculating within the canyon. At 350 m depth, upwelling was not occurring.

Effect of canyon circulation on zooplankton distributions

Except for the strongly migratory euphausiids, the distributions of the zooplankton species in the vicinity of the canyon were consistent with passive advection by the currents around the canyon. Species resident deeper in the water column were displaced towards the head of the canyon, particularly on the downstream side of the canyon, consistent with the flow observed at 150 m.

Shallow nonmigrators

Species that were found only in the upper 50-m depth stratum both day and night were generally found at the same cross-shore location over the canyon as they are in other places along the southern shelf. *Acartia longiremis*, a shelf species, was found primarily at station B2 in the region of the eddy. The eddy was weak near the surface and probably was not able to trap tracers. This difference could be explained by the fact that the flow in this region was more seaward than at station D2 downstream.

Oikopleura spp. and *Oithona* spp. (but mostly *spinifera*) were found primarily at the mouth of the canyon. As these are shelf-to-shelf-edge and shelf-edge-to-oceanic species, their distribution over the canyon appears to be similar to that away from the canyon.

Paracalanus parvus was found primarily at the mouth of the canyon. In contrast with most of the other zooplankton species described here, *Paracalanus* is at or near the northern limit of its range. Although its distribution is nearshore at the centre of its latitudinal range (off California), an outer shelf slope maximum is the early summer norm off British Columbia. Abundance off southern British Columbia (anomalously high in the mid- to late 1990s, e.g., Mackas et al. 2001) is associated with poleward transport of warmer water from the California and Oregon continental margins. The strongest poleward transport of southerly water is by the winter wind-forced Northeast Pacific Coastal Current (Thomson and Gower 1998), the axis of which is centred along and slightly seaward of the British Columbia shelf break. During the summer growing season, the *Paracalanus* population gradually spreads shoreward from this initial offshore maximum. Euphausiid calyptopis larvae were patchy around the canyon and showed no clear geographical preference.

Deep nonmigrators

Neocalanus plumchrus is a subarctic oceanic species that has a strong seasonal ontogenetic vertical migration (Miller and Clemons 1988) but weak or no diel vertical migration (Mackas et al. 1993). By July, the bulk of its population was dormant stage 5 copepodites, normally located in depth strata 400–700 m. In our canyon samples, *N. plumchrus* was found only at the two mouth stations and at station D2, the station downstream of the head. The presence of *N. plumchrus* at D2 could be a consequence of the deep up-canyon flow, which brings oceanic water up canyon and then perhaps onto the shelf.

Oceanic species *Eukrohnia hamata* was found primarily at the downstream station at the mouth of the canyon. This distribution could reflect a pattern similar to that of *N. plumchrus* but shifted offshore. As flow at the downstream stations is primarily onshore, species usually further offshore than the shelf edge could be advected into the vicinity of station D4. Such a pattern would suggest that *N. plumchrus* should be more abundant at station D4 as well; during the day tow, it was not, but during the night tow, it was more abundant.

The oceanic chaetognath *Sagitta scrippsae* was observed at all stations in about equal numbers. Like *Paracalanus*, *S. scrippsae* is near the northern limit of its latitudinal range, and high abundance indicates poleward transport of warm water. Unlike *Paracalanus*, its vertical distribution is centred deep in the water column. Off British Columbia, it is normally found in deep tows from locations seaward of the continental shelf. Presence of this species at the head of the canyon therefore implies a shift shorewards compared with its general distribution.

Calanus marshallae, a shelf species, was found at the head of the canyon with no upstream/downstream asymmetry. Like *N. plumchrus*, most of the July population was dormant (and deep) stage 5 copepodites.

Mixed-depth migrators

Sagitta elegans, a shelf-edge-to-shelf species, was found at all stations, implying a distribution over the canyon similar to that over the southern shelf in general.

Deep migrators

The larger bodied, strongly migratory adults and late juveniles of both euphausiid species *Euphausia pacifica* and *Thysanoessa spinifera* were most abundant in the eddy region, near the head of the canyon. This in-canyon similarity of distribution is an interesting result because their larger scale distributions are quite different. Specifically, *T. spinifera* is a shelf species confined to the eastern margin of the North Pacific, while *E. pacifica* is a shelf-break-to-oceanic species with a trans-Pacific distribution extending along the southern margin of the subarctic gyres (see Brinton 1962; Mackas and Tsuda 1999).

The oceanic species *Metridia pacifica* had a distribution similar to that of *E. hamata* and was found primarily at station D4, on the downstream side of the canyon near the mouth. Both of these species spend daylight hours well below the surface layer (75–400 m) but differ in their night vertical distribution. *Metridia* migrates up into the surface layer to feed, while *Eukrohnia* remains mostly below 100 m.

In summary, except for the euphausiids, the observed zooplankton distribution of all major species was consistent with passive advection by the currents. The strong onshore flow at 150 m depth caused a shoreward shift of the distribution of deep zooplankton by about the length of the canyon.

Dynamics and consequences of the rim depth eddy

Strong cyclonic vorticity has been observed and modeled at canyon rims. Hickey (1997) observed cyclonic vorticity as strong as $0.6f$ at the rim of Astoria Canyon, where f is the Coriolis frequency. During relaxation from upwelling, a cyclonic eddy was observed. The strong vorticity was explained by stretching of shelf water as it passes over the canyon. Numerical models have simulated strong vorticity but not a closed eddy. Thus, two dynamical questions remain: what causes the stretching and is the generated vorticity strong enough to cause a closed eddy?

Shelf water is observed to descend into the canyon as it crosses the canyon. The data from Barkley Canyon show that the 26.4 sigma-*t* surface dips down into the canyon. Isopycnal descent over Astoria Canyon using nepheloid layers as tracers is seen in fig. 12*a* of Hickey (1997).

The explanation for the shelf-water descent into the canyon lies in a consideration of the dynamics of the layer below the flow crossing the canyon. Consider the situation of a southward shelf-break current starting from rest. Initially, the isopycnals are everywhere flat. As the shelf-break current starts, due to wind forcing or propagation of continental shelf waves, the isopycnals tilt up towards the coast so that the current is in approximate geostrophic balance. The alongshore shelf-break current implies a cross-shelf pressure gradient with lower pressure near the coast. Over the canyon, the flow above the rim of the canyon crosses the canyon. Within the canyon, the initial response to the cross-shore pressure gradient (before one inertial period) causes the current to flow up canyon towards the head. However, this flow turns to the right due to the Coriolis force and tends to flow across the canyon similar to the flow just above it. Flow away from the northern (upstream) canyon wall causes depression of the isopycnals at the upstream canyon wall. Sinking of the isopycnals tends to reduce the pressure within the canyon at the upstream wall. This in turns creates a cross-canyon pressure gradient and reduces the flow away from the wall. After an inertial period, the lower pressure at

the upstream wall causes flow up canyon, increasing the pressure there and again (geostrophically this time) decreasing the flow away from the upstream wall but leaving a marked cross-canyon tilt to the isopycnals. The flow above the rim deepens and fills the space left by the depressed isopycnals below the rim. In effect, as flow moves over the canyon from the upstream wall, it "falls" into the canyon.

Given the observed isopycnal stretching, one can estimate the stretching vorticity (Hickey 1997). Subtracting the height of the 26.3 isopycnal surface from the 26.5 isopycnal surface, we observe stretching of a factor of almost 2 (21–35 m), similar to the results over Astoria Canyon. If we assume that the upstream flow has no relative vorticity, we can estimate the vorticity within the canyon using conservation of potential vorticity:

$$(2) \qquad PV = \frac{\zeta + f}{h}$$

where ζ is the relative vorticity, f is the planetary vorticity, assumed uniform on the scale of the canyon, and h is the vertical thickness between two isopycnals. The observed stretching (21–35 m) implies a vorticity of 1.7f, which is larger than the value of 0.3f computed by the diagnostic model. This overestimation of the vorticity is expected, as conservation of potential vorticity neglects all dissipation mechanisms.

A simple estimation of the generated eddy was made by simplifying the observed upstream thickness as

h(B2), y = 0 km

h(B3), y = 8.3 km

h(B4), y = 16.7 km

h(A4), $y \geq$ 25.0 km

where h is the depth between the two isopycnals at a station and y increases offshore. Linear interpolation was used between the points given above.

The over-canyon thickness was specified at the same y positions as that upstream but using stations C2, C3, C4, and A4. The domain is taken from the 150-m isobath out 100 km. A flux of 37×10^3 $m^3 \cdot s^{-1}$ (equivalent to 3 $cm \cdot s^{-1}$ over 100 km through a layer 12.4 m deep) is assumed to flow through this section. Inversion of the vorticity to velocity is performed by relaxation (Press et al. 1986). The result is a large, strong eddy centred over the canyon. The estimated eddy is about a factor of 2 stronger than the observed eddy and is located further towards the mouth of the canyon. This overestimation is expected, as all dissipation mechanisms are neglected.

Published prognostic models (as opposed to the diagnostic numerical model described in the Results section above) have not predicted such an eddy. This omission is caused by the lack of stretching generated in the models due to too-smooth topography (Klinck 1996) or use of a layer model with thick layers (Allen 1996). A smooth, Gaussian-style canyon is much narrower towards the head than the mouth. This shape of canyon generates significantly less stretching than a more rectangular canyon such as Astoria Canyon or Barkley Canyon (Allen et al. 1999). The simple demonstration given here illustrates that the models will reproduce the eddy once the stretching is correct. Klinck et al. (1999) numerically simulated such an eddy.

Fig. 8. Results from the Lagrangian tracer simulations at 150 m depth. The tracers were tracked in the flow calculated by the diagnostic model using the observed density field and averaged winds from the weather buoy. The four major tidal constituents were included. (*a*) Initial positions of the tracers. Open circles (solid circles) mark tracers that were advected out of (retained within) the domain over the 10-day simulation. (*b*) Position of the retained tracers after 10 days. All retained tracers are in the eddy region near station B2.

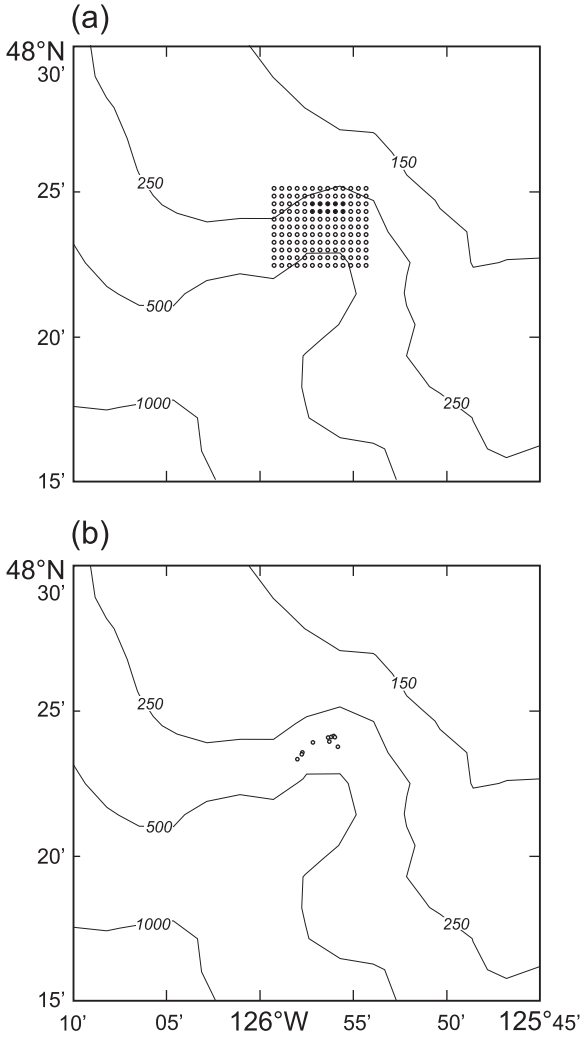

As the eddy is 10 km wide compared with the tidal excursion of 0.9 km and has a current speeds of 20 $cm \cdot s^{-1}$, as compared with the barotropic tidal current of 2 $cm \cdot s^{-1}$, it is expected to trap tracers (at 150 m) in a Lagrangian sense (Foreman et al. 1992). Eddies and other recirculating flows can trap passive tracers but do not aggregate them. However, the euphausiid species *E. pacifica* and *T. spinifera* were observed to be aggregated in the eddy region. Although flow in the ocean is nondivergent in three dimensions, there can be regions of horizontal convergence (divergence). As the euphausiids can maintain their preferred depth against the weak vertical velocities, they can be aggregated by horizontal convergence. Examples are given in Mackas et al. (1997)

and Simard et al. (1996) where euphausiids are seen to aggregate in regions of strongly sloping bottom topography due to flow toward the slope.

Regions of strong convergence are seen at depths occupied by euphausiids during the day. Euphausiids have been shown to aggregate at the shelf edge upstream of the canyon at about 100 m depth (Mackas et al. 1997). Using our diagnostic model, the horizontal convergence $-(\partial u/\partial x+\partial v/\partial y)$ at 100 m was calculated. (Here, u and v are the horizontal velocity components in the x and y direction, respectively). Very strong regions of convergence occur particularly in the region where the eddy flow crosses the downstream rim. The horizontal convergence at 100 m shows stronger convergence at B2 than at the other three rim stations. Backward trajectories of 5-h length were constructed. Only zooplankton caught at B2 passed through a convergence zone just before being trapped. The observations show that the shelf-to-shelf-edge species *T. spinifera* aggregated strongly at B2. The shelf-edge-to-oceanic species *E. pacifica* had twice the numbers at B2 as at D2.

In order to test the retention characteristics of the eddy, several Lagrangian tracer simulations were carried out using the diagnostic model. Tracers were released over a 6 × 5 km horizontal grid centred over the eddy and tracked for 10 days. Release depths were 50, 150, 250, and 350 m, respectively. Due to the strong shelf-break current, all the tracers released at 50 m moved southwesterly away from Barkley Canyon. However, at all other depths, some of the tracers were retained within the eddy. More tracers starting at 250 m were retained than at the other depths, and in all cases (after 10 days), the tracers had moved to the northeast side of the canyon head and were at depths between 90 and 130 m above the bottom. Figure 8*a* shows the grid of initial grid seedings and the locations that were trapped in the eddy when released at 150 m depth. Figure 8*b* shows the locations of these trapped drogues after 10 days. Further experiments revealed that the precise release time relative to tidal flood, ebb, spring, or neap currents, made very little difference. Thus, it appears that the eddy both traps and converges passive tracers.

In summary, the west coast of Vancouver Island experienced weak upwelling in 1997 probably due to the effects of the 1997–1998 El Niño. The GLOBEC cruise at the end of July took place at a time of weak upwelling-favourable winds and a southeastward shelf-break current. Enhanced upwelling and onshore flow were observed through Barkley Canyon.

Water properties showed enhanced upwelling at the thermocline down to a depth of about 200 m. Observations of canyon effects so close to the surface are new, although they are unlikely unique to Barkley Canyon. Below 200 m, the isopycnals are bowl-shaped, dipping in the centre of the canyon. The spreading isopycnals over the canyon imply water column stretching (and thus cyclonic vorticity) over the canyon. The near-surface flow is generally across the canyon. Deeper, near rim level, the flow turns up the canyon as it crosses the north rim of the canyon. The flow crosses the south rim of the canyon turning to join the southeastward flow. Thus, the canyon shifts the shelf-break current shorewards. At the head towards the north side of the canyon, a strong eddy forms. This eddy is consistent with vorticity generated by the observed vortex stretching. Deeper in the canyon, the flow turns cyclonically.

Most zooplankton are simply advected by the currents. Those near the surface are carried across the canyon with little deflection from their normal cross-shelf position. Those deeper are advected shorewards by the currents through the canyon. Euphausiids are aggregated near the head of the canyon due to the strong horizontal convergence associated with the eddy.

Acknowledgments

The authors extend their thanks to the crew and scientists of the CCGS *John P. Tully* during the west coast GLOBEC cruise of July 1997. Steve Romaine carried out most of the zooplankton net tow sampling. Moira Galbraith identified and counted the zooplankton. This is a contribution of GLOBEC cosponsored by the Natural Sciences and Engineering Research Council of Canada and Fisheries and Oceans Canada.

References

Allen, S.E. 1996. Topographically generated, subinertial flows within a finite length canyon. J. Phys. Oceanogr. **26**: 1608–1632.

Allen, S.E., Dinniman, M.S., Klinck, J.M., and Hickey, B.M. 1999. Dynamics of advection-driven upwelling over a submarine canyon. EOS, **80**(49): OS221. (Abstr.)

Blanton, B.O. 1992. User's manual for 3-dimensional drogue tracking on a finite element grid with linear elements. Release 95.1. Ocean Processes Numerical Methods Laboratory, University of North Carolina at Chapel Hill, Chapel Hill, N.C.

Brinton, E. 1962. The distribution of pacific euphausiids. Bull. Scripps Inst. Oceanogr. Univ. Calif. No. 8.

Crawford, W.R., and Dewey, R.K. 1989. Turbulence and mixing: sources of nutrients on the Vancouver Island continental shelf. Atmos.–Ocean, **27**: 428–442.

Foreman, M.G.G., Bapista, A.M., and Walters, R.A. 1992. Tidal model studies of particle trajectories around a shallow coastal bank. Atmos.–Ocean, **30**: 43–69.

Foreman, M.G.G., Thomson, R.E., and Smith, C.L. 2000. Seasonal current simulations for the western continental margin of Vancouver Island. J. Geophys. Res. **105**: 19 665 – 19 698.

Freeland, H.J., and Denman, K.L. 1982. A topographically controlled upwelling center off southern Vancouver Island. J. Mar. Res. **40**: 1069–1093.

Freeland, H.J., and Thomson, R. 1999. The El Niño signal along the west coast of Canada — temperature, salinity and velocity. *In* Proceedings of the 1998 Science Board Symposium on the Impacts of the 1997/98 El Niño Event on the North Pacific Ocean and its Marginal Seas. PICES Sci. Rep. No. 10. *Edited by* H.J. Freeland, W.T. Peterson, and A. Tyler. North Pacific Marine Science Organization, Sidney, B.C. (url: http://pices.ios.bc.ca/picespub/reports/report99.htm)

Hickey, B.M. 1997. The response of a steep-sided narrow canyon to strong wind forcing. J. Phys. Oceanogr. **27**: 697–726.

Hickey, B.M., Baker, E., and Kachel, N. 1986. Suspended particle movement in and around Quinault Submarine Canyon. Mar. Geol. **71**: 35–83.

Klinck, J.M. 1996. Circulation near submarine canyons: a modeling study. J. Geophys. Res. **101**: 1211–1223.

Klinck, J.M., Hickey, B.M., Dinniman, M.S., and Allen, S.E. 1999. Model-data comparison of flow over realistic topography in a region with coastal submarine canyons. EOS, **80**(49): OS221. (Abstr.)

Lynch, D.R., Werner, F.E., Greenberg, D.A., and Loder, J.W. 1992. Diagnostic model for baroclinic, wind-driven and tidal circulation in shallow seas. Continental Shelf Res. **12**(1): 507–533.

Lynch, D.R., Ip, J.T.C., Naimie, C.E., and Werner, F.E. 1996. Comprehensive coastal circulation model with application to the Gulf of Maine. Continental Shelf Res. **16**(7): 875–906.

Mackas, D.L. 1992. Seasonal cycle of zooplankton off southwestern British Columbia. Can. J. Fish. Aquat. Sci. **49**: 903–921.

Mackas, D.L., and Tsuda, A. 1999. Mesozooplankton in the eastern and western subarctic Pacific: community structure, seasonal life histories, and interannual variability. Prog. Oceanogr. **43**: 335–363.

Mackas, D.L., Louttit, G.C., and Austin, M.J. 1980. Spatial distribution of zooplankton and phytoplankton in British Columbia coastal waters. Can. J. Fish. Aquat. Sci. **37**: 1476–1487.

Mackas, D.L., Sefton, H., Miller, C.B., and Raich, A. 1993. Vertical habitat partitioning by large calanoid copepods in the oceanic subarctic Pacific during spring. Prog. Oceanogr. **32**: 259–294.

Mackas, D.L., Kieser, R., Saunders, M., Yelland, D.R., Brown, R.M., and Moore, D.F. 1997. Aggregation of euphausiids and Pacific hake (*Merluccius productus*) along the outer continental shelf off Vancouver Island. Can. J. Fish. Aquat. Sci. **54**: 2080–2096.

Mackas, D.L., Thomson, R.E., and Galbraith, M. 2001. Changes in the zooplankton community of the British Columbia continental margin, 1985–1999, and their covariation with oceanographic conditions. Can. J. Fish. Aquat. Sci. **58**: 685–702.

Macquart-Moulin, C., and Patriti, G. 1996. Accumulation of migratory micronekton crustaceans over the upper slope and submarine canyons of the northwestern Mediterranean. Deep-Sea Res. **43**: 579–601.

Miller, C.B., and Clemons, M. 1988. Revised life history analysis for large grazing copepods in the subarctic Pacific Ocean. Prog. Oceanogr. **20**: 293–313.

Naimie, C.M., Loder, J.W., and Lynch, D.R. 1994. Seasonal variation of the three-dimensional residual circulation on Georges Bank. J. Geophys. Res. **99**: 15 967 – 15 989.

Pereyra, W.T., Pearcy, W.G., and Carvey, F.E.J. 1969. *Sebastodes flavidus*, a shelf rockfish feeding on mesopelagic fauna, with consideration of the ecological implications. J. Fish. Res. Board Can. **26**: 2211–2215.

Peterson, W.T., Miller, C.B., and Hutchinson, A. 1979. Zonation and maintenance of copepod populations in the Oregon upwelling zone. Deep-Sea Res. **26**: 467–494.

Press, W.H., Flannery, B.P., Teukolsky, S.A., and Vetterling, W.T. 1986. Numerical recipes: the art of scientific computing. Cambridge University Press, Cambridge, U.K.

Simard, Y., de Ladurantye, R., and Therriault, J.-C. 1996. Aggregation of euphausiids along a coastal shelf in an upwelling environment. Mar. Ecol. Prog. Ser. **32**: 203–215.

Smith, C.L., Hill, A.E., Foreman, M.G.G., and Peña, M.A. 2001. Horizontal transport of marine organisms resulting from interactions between diel vertical migration and tidal currents off the west coast of Vancouver Island. Can. J. Fish. Aquat. Sci. **58**: 736–748.

Thomson, R.E., and Gower, J.F.R.1998. A basin-scale oceanic instability event in the Gulf of Alaska. J. Geophys. Res. **103**: 3033–3040.

Thomson, R.E., and Ware, D.M. 1996. A current velocity index of ocean variability. J. Geophys. Res. **101**: 14 297 – 14 310.

Thomson, R.E., Hickey, B.M., and LeBlond, P.H. 1989. The Vancouver Island coastal current: fisheries barrier and conduit. *In* Effects of ocean variability on recruitment and an evaluation of parameters used in stock assessment models. *Edited by* R. Beamish and G.A. McFarlane. Can. Spec. Publ. Fish. Aquat. Sci. No. 108. pp. 265–296.

Whitehead, H., Faucher, A., Gowans, S., and McCarrey, S. 1997. Status of the northern bottlenose whale, *Hyperoodon ampullatus*, in the Gully, Nova Scotia. Can. Field-Nat. **111**: 287–292.